

## Conducting two-phase silicon oxide layers for thin-film silicon solar cells

Peter Buehlmann<sup>1</sup>, Julien Bailat<sup>2</sup>, Andrea Feltrin<sup>1</sup>, Christophe Ballif<sup>1</sup>

<sup>1</sup>IMT, University of Neuchâtel, Neuchâtel, Switzerland

<sup>2</sup> Now at Oerlikon Solar-Lab, Neuchâtel, Switzerland

### ABSTRACT

We present optical properties and microstructure analyses of hydrogenated silicon sub-oxide layers containing silicon nanocrystals (nc-SiO<sub>x</sub>:H). This material is especially adapted for the use as intermediate reflecting layer (IRL) in micromorph silicon tandem cells due to its low refractive index and relatively high transverse conductivity. The nc-SiO<sub>x</sub>:H is deposited by very high frequency plasma enhanced chemical vapor deposition from a SiH<sub>4</sub>/CO<sub>2</sub>/H<sub>2</sub>/PH<sub>3</sub> gas mixture. We show the influence of H<sub>2</sub>/SiH<sub>4</sub> and CO<sub>2</sub>/SiH<sub>4</sub> gas ratios on the layer properties as well as on the micromorph cell when the nc-SiO<sub>x</sub>:H is used as IRL. The lowest refractive index achieved in a working micromorph cell is 1.71 and the highest initial micromorph efficiency with such an IRL is 13.3 %.

### INTRODUCTION

Thin film silicon technologies have a high potential for further cost reduction of terrestrial photovoltaics for energy production. In this technology, multi-junction solar cells are candidate to achieve efficiencies comparable to the well established crystalline silicon solar cells. One of the most promising structures is the micromorph cell where a high band-gap amorphous top cell and a low band-gap microcrystalline bottom cell are stacked upon each other to better exploit the solar spectrum. The individual cells composing a multi-junction cell are electrically connected in series and special care has therefore to be taken to match their currents. Matching of currents can be achieved by adjusting the thickness of the thin absorber layers or by the insertion of an intermediate reflecting layer (IRL). The second solution is especially interesting for the micromorph cell where the top cell has to be kept reasonably thin (< 300 nm) to limit the effects of the light induced Staebler-Wronski degradation of the amorphous material [1]. For high reflectivity, the IRL should have a refractive index (n) as low as possible whereas for the electrical requirements, the IRL must have a transverse conductivity of at least 10<sup>-5</sup> S/cm to avoid blocking the device. Very low in-plane conductivity is desired to avoid series interconnection of shunts in the elementary cells. The first results on micromorph cells with IRL were presented in 1996 by D. Fischer [2] who used ZnO as low-n material. Later a different approach was introduced by K. Yamamoto [3] without specifying the material used. In this study we will investigate on the use of n-doped, hydrogenated silicon sub-oxide containing silicon nanocrystals (nc-SiO<sub>x</sub>:H) as proposed by our group [4] and A. Lambertz [5] in 2007.

### EXPERIMENTAL DETAILS

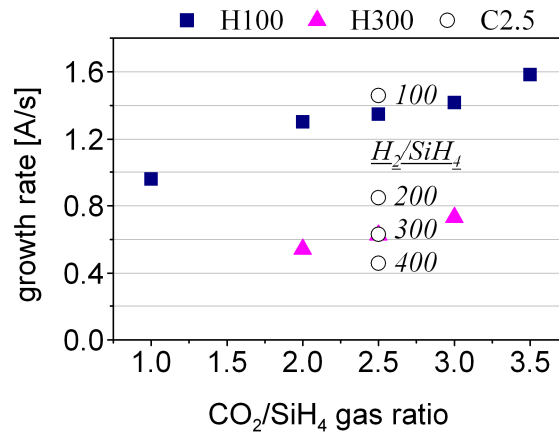
The n doped nc-SiO<sub>x</sub>:H films were prepared from a mixture of SiH<sub>4</sub>, CO<sub>2</sub>, H<sub>2</sub> and PH<sub>3</sub> gases in a capacitively coupled very high frequency plasma enhanced chemical vapor deposition (VHF-PECVD) system. In this study all the SiO<sub>x</sub> layers were deposited at a pressure of 0.7 mbar,

at a frequency of 110 MHz, with a power density of 0.1 W/cm<sup>2</sup>, a constant PH<sub>3</sub>/SiH<sub>4</sub> gas ratio of 0.1 and a deposition time sufficient to reach a layer thickness of ~ 90 nm. Ellipsometry, Raman scattering and thickness measurements were performed on layers deposited on glass. Refractive index (n) was found from fitting the ellipsometry measurements to a Tauc-Lorentz dispersion model including a surface roughness layer. The thickness was measured with a height profiler. Infrared (IR) absorption measurements were performed with a Nicolet 8700 system from Thermo on samples deposited on intrinsic, one-side polished wafers. The absorption spectra were normalized with the layer thickness.

The amorphous and microcrystalline cells were prepared by PECVD. Glass covered with rough CVD ZnO was used as substrate for the micromorph cells. CVD ZnO was used as back contact and teflon as diffusive back reflector. The cells were fully patterned to a size of 1.2 cm<sup>2</sup>. The short-circuit current density (J<sub>sc</sub>) of the solar cells was calculated from the measurement of the external quantum efficiency (EQE) curve, by integrating, over the wavelength range from 350 to 1100 nm, the product of EQE times the incoming photon flux of the AM1.5g solar spectrum. The current–voltage curves were measured under a dual lamp WACOM solar simulator in standard test conditions (25 °C, AM1.5g spectrum, and 1000 W/m<sup>2</sup>).

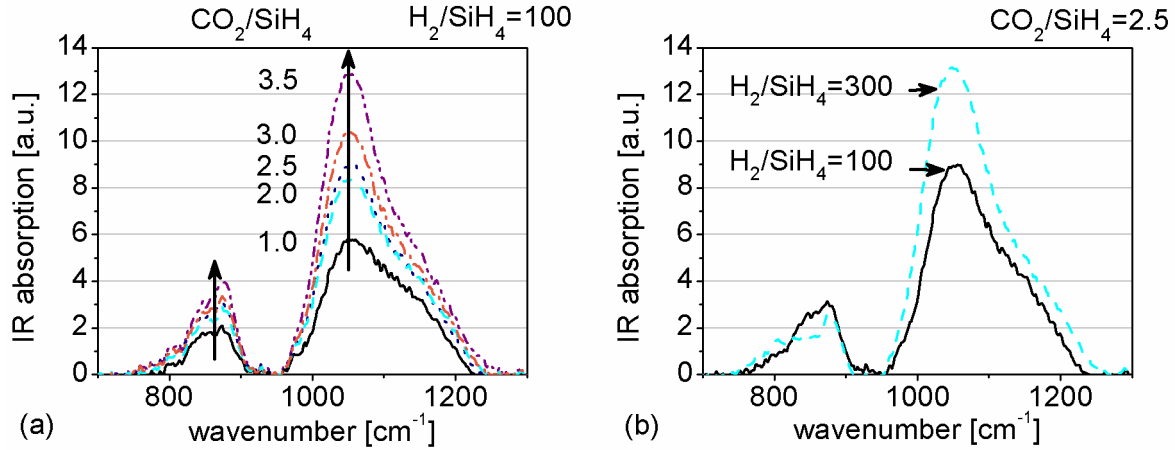
## RESULTS

In this study, we present nc-SiO<sub>x</sub> layers from three different gas ratio series. In the series H100 and H300, we varied the CO<sub>2</sub>/SiH<sub>4</sub> between 1 and 3.5 with a constant H<sub>2</sub>/SiH<sub>4</sub> gas flow ratio of 100 and 300 respectively. In series C2.5, the H<sub>2</sub>/SiH<sub>4</sub> was varied from 100 to 400 with a constant CO<sub>2</sub>/SiH<sub>4</sub> gas ratio of 2.5. Figure 1 compares the growth rates of all the nc-SiO<sub>x</sub> layers from these three series.



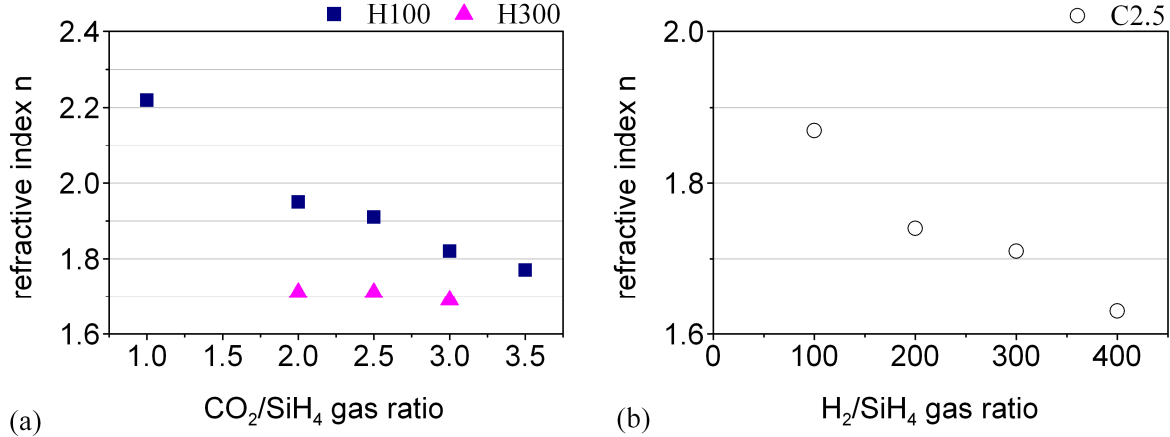
**Figure 1.** Growth rates of nc-SiO<sub>x</sub> layers from the three series: H100, H300 and C2.5

Figure 2a shows the IR absorption spectra of the H100 series. The peaks at ~ 1050 cm<sup>-1</sup> and between 800 and 900 cm<sup>-1</sup> which have been reported to stem from the Si-O-Si stretching and bending modes [6, 7] increase with increasing CO<sub>2</sub>/SiH<sub>4</sub> gas ratio. The oxygen content increases in a similar manner when the H<sub>2</sub>/SiH<sub>4</sub> is increased from 100 to 300 with a fixed CO<sub>2</sub>/SiH<sub>4</sub> of 2.5 as it can be seen on figure 2b.



**Figure 2.** Infrared absorption spectra of the H100 series (a) and the comparison of two spectra with  $\text{CO}_2/\text{SiH}_4$  gas ratio of 2.5 but different  $\text{H}_2/\text{SiH}_4$  gas ratios (b).

Figure 3a and 3b show the refractive index of the nc- $\text{SiO}_x$  layers as a function of  $\text{CO}_2/\text{SiH}_4$  and  $\text{H}_2/\text{SiH}_4$  gas ratios. For the series H100 and H300, the  $n$  decreases with increasing  $\text{CO}_2/\text{SiH}_4$  gas ratio. The same effect is also observed for the C2.5 series with increasing  $\text{H}_2/\text{SiH}_4$  gas ratio. This tendency has been described by Iftiqar [6] who suggested that the main mechanism of oxygen incorporation in  $\text{SiO}_x$  films deposited by PECVD is through the formation of O-H complexes in the plasma which more easily get to the growing layer surface than the highly reactive and electronegative atomic oxygen.



**Figure 3.** Refractive index ( $n$ ) of nc- $\text{SiO}_x$  layers from the series: H100, H300 (a) and C2.5 (b)

To gain further insight into structural properties of the nc- $\text{SiO}_x$  layers we performed Raman scattering measurements and calculated the Raman crystalline fraction in the silicon phase [8]. Since the measurements don't account for the  $\text{SiO}_2$ , which is the dominant phase in our layers, the signal represents in this case not a crystalline volume fraction of the layer, but only the ratio of crystalline silicon signal over the crystalline plus amorphous silicon signal. The Raman scattering signal is very noisy because there is only little silicon phase remaining in our films. Figure 4a shows the Raman spectra of the H100 series. Figure 4b and 4c show the calculated Raman crystalline fraction in the silicon phase, and the total Raman silicon signal intensity as a function of  $\text{CO}_2/\text{SiH}_4$  gas ratio for the H100 and H300 series. The crystalline

fraction decreases with increasing  $\text{CO}_2/\text{SiH}_4$  gas ratio whereas the total silicon Raman signal intensity remains almost constant. The total Raman peak intensity of the H100 series is almost twice as high as for the series H300 for comparable crystalline fractions. Based on these data, increasing  $\text{CO}_2/\text{SiH}_4$  seems to convert the crystalline silicon to amorphous silicon without reducing the presence of the silicon phase whereas an increased  $\text{H}_2/\text{SiH}_4$  seems to reduce the presence of silicon phase significantly.

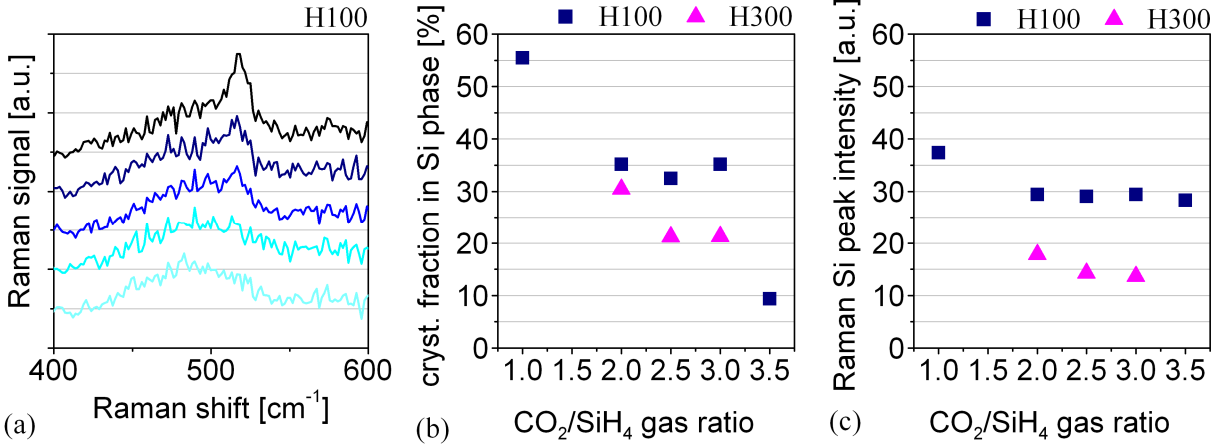


**Figure 4.** Raman spectra of the H100 series (a), Raman crystalline fraction in the silicon phase (b) and total Raman silicon peak intensity (c) of the H100, H300 and C2.5 series.

## DISCUSSION

When the nc- $\text{SiO}_x$  layers are used as intermediate reflectors in micromorph cells, a sufficiently high transverse conductivity is needed to avoid blocking the device. If a 100 nm thick layer should not increase the series resistance in the micromorph cell more than  $1 \text{ Ohm}\cdot\text{cm}^2$ , we can calculate a lower limit of the conductivity of  $10^{-5} \text{ S/cm}$ . On all the layers presented above we measured in-plane conductivities below this value. Figure 5 shows the current density-voltage (JV) curves of top-limited micromorph cells with the nc- $\text{SiO}_x$  layers from the H100 and the H300 series.  $J_{\text{sc}}$  increases with decreasing  $n$  of the silicon oxide based intermediate reflector (SOIR) and there are cells with no increase of series resistance due to the SOIR with  $n$  as low as 1.71 although the measured in-plane conductivity of most  $\text{SiO}_x$  layers is below  $10^{-10} \text{ S/cm}$ , which is the lower limit of our measurement system. From figure 4 we can assume that the in-plane conductivity is mostly determined by the highly resistive amorphous  $\text{SiO}_x$  matrix whereas we believe that silicon nanocrystals are responsible for a relatively high transverse conductivity as observed in the micromorph cells.

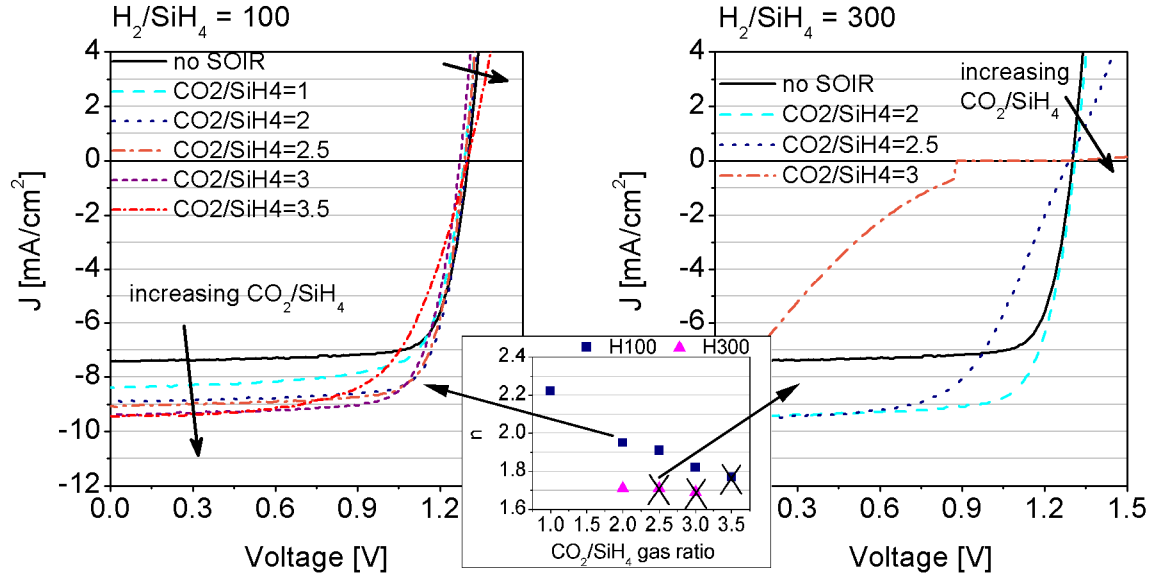


**Figure 5.** J-V curves of top-limited micromorph solar cells with the different SOIR from the H100 and H300 series. The inset shows the refractive index of the SOIR. SOIR that caused an increase of series resistance in cell are marked with a cross).

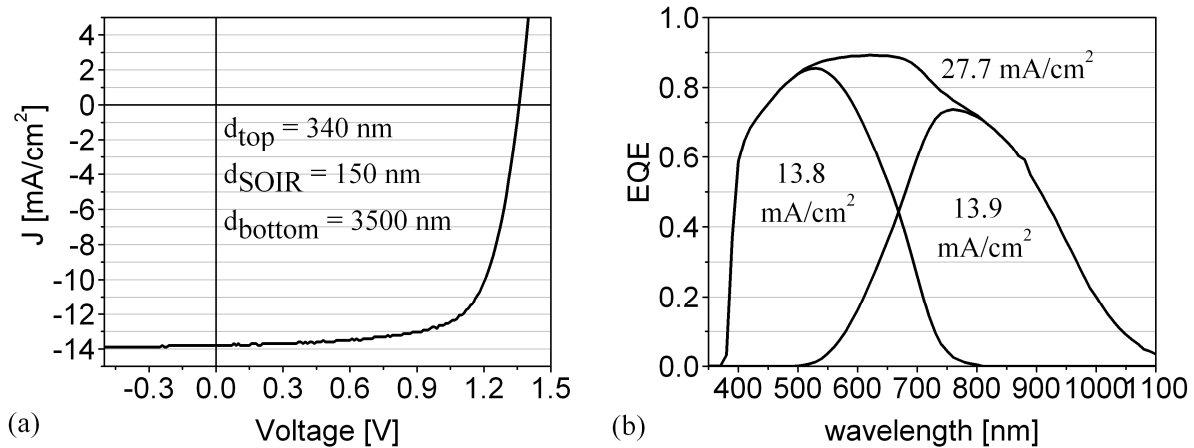


**Figure 6.** J-V (a) and EQE (b) curves of micromorph cell with 13.3 % initial efficiency (Cell fully patterned to 1.2 cm<sup>2</sup>; with broadband anti-reflection coating on glass;  $V_{oc} = 1.36$  V, FF = 70.8,  $J_{sc} = 13.8$  mA/cm<sup>2</sup>)

The SOIR with the lowest refractive index ( $n = 1.71$ ) without deteriorating the series resistance of the micromorph cell is deposited with  $CO_2/SiH_4 = 2$  and  $H_2/SiH_4 = 300$ . Figure 6 shows an optimized micromorph cell, where the use of a SOIR has lead to a best initial efficiency of 13.3 % with top cell, SOIR, bottom cell thicknesses of 340, 150, 3500 nm respectively [9].

## CONCLUSIONS

We presented in this study nc-SiO<sub>x</sub> layers with refractive indexes as low as 1.71 that can be used as SOIR in micromorph cells without compromising its series resistance. From optical

measurements of the layers and from the results of the same layers incorporated as intermediate reflectors in micromorph cells we conclude that the high H<sub>2</sub> dilution is important to get low refractive index material with sufficiently high transversal conductivity. Finally we showed an optimized micromorph cell with an initial efficiency of 13.3 % with top cell, SOIR, bottom cell thicknesses of 340, 150, 3500 nm respectively.

## ACKNOWLEDGMENTS

The authors gratefully acknowledge the support of the Swiss Federal Energy Office (OFEN) (project 101191) and the EU (Athlet Project, contract 019670).

## REFERENCES

1. M. S. Bennett, J. L. Newton, and K. Rajan, Proceedings of the 7th European Photovoltaic Solar Energy Conference, Sevilla, Spain (Reidel, Dordrecht, 1987), pp. 544-548.
2. D. Fischer et al. in proceedings of the 25th IEEE Photovoltaic Specialists Conference, Washington D. C., USA (IEEE, New York, 1996), pp. 1053-1056.
3. K. Yamamoto et al., Solar Energy **77** (2004) pp. 939-949.
4. P. Buehlmann et al., Appl. Phys. Lett. **91**, 143505 (2007).
5. A. Lambertz et al., 22th European Photovoltaic Solar Energy Conference, Milan, Italy (WIP, Munich, 2007), pp. 1839-1842.
6. S. M. Iftiquar, J. Phys. D: Appl. Phys. **31**, 1630 (1998); High Temperature Material Processes, **6** (2002)
7. G. Lucovsky et al., Phys. Rev. B **28**, 3225 (1983); Sol. En. Mat. **8**, 165 (1982).
8. C. Droz, E. Vallat-Sauvain, J. Bailat, L. Feitknecht, and A. Shah, Proceedings of 17th European Photovoltaic Solar Energy Conference, Munich, Germany (WIP, Munich, 2002), pp. 2917-2920.
9. D. Dominé et al., 23th European Photovoltaic Solar Energy Conference, Valencia, Spain (WIP, Munich, 2008), pp. 2091-2095.